SUPPLEMENTARY MATERIAL

CRUST DEVELOPMENT INFERRED FROM NUMERICAL MODELS OF LAVA FLOW AND ITS SURFACE THERMAL MEASUREMENTS

Igor Tsepelev[1], Alik Ismail-Zadeh[2,3], Yulia Starodubtseva[1], Alexander Korotkii [1,4], Oleg Melnik[5]

[1] *Institute of Mathematics and Mechanics, Russian Academy of Sciences, Yekaterinburg, Russia*
[2] *Institute of Applied Geosciences, Karlsruhe Institute of Technology, Karlsruhe, Germany*
[3] *Institute of Earthquake Prediction Theory and Mathematical Geophysics, Russian Academy of Sciences, Moscow, Russia*
[4] *Institute of Natural Sciences and Mathematics, Ural Federal University, Yekaterinburg, Russia*
[5] *Institute of Mechanics, Lomonosov Moscow State University, Moscow, Russia*

S1 Influence of linear and nonlinear heat flow at the interface between a lava and the atmosphere

Problem (1)-(14) with the boundary condition (15) for linear heat flow and condition (16) for nonlinear heat flow is solved numerically. Dimensionless parameters used in Eqs. (15) and (16) are Nu = 4, a_1=2.593, and a_2=18.911. Numerical experiments have been performed for three dimensionless injection rates, and the dimensionless injection temperature is 4.4. The lava viscosity varies within six orders of magnitude, and $\eta_0 = 10^6$.

Figures S1a, S1b, and S1c presents the magnitude of the dimensionless values of the lava velocity (upper panels in each figure), the viscosity (middle panels), and the lava temperature (lower panels). At higher dimensionless injection rates ($|\mathbf{u}_1| = 10^{-2}$, Fig. S1a) and temperature advection with the flow, the lava temperature takes the value of the injection temperature almost in the entire model domain. The crust (the red part of the model domain seen in the viscosity panels of Fig. S1a, as well as S1b and S1c) is thin in both cases of the linear (the left panels) and nonlinear (the right panels) heat flow at the upper surface of the model domain, although the crust is relatively thicker in the case of the nonlinear heat flow. At lower injection rates of 10^{-3} (Fig. S1b) and 10^{-4} (Fig. S1c), the crust becomes thicker and especially in the case of nonlinear heat flow.

Linear heat flow

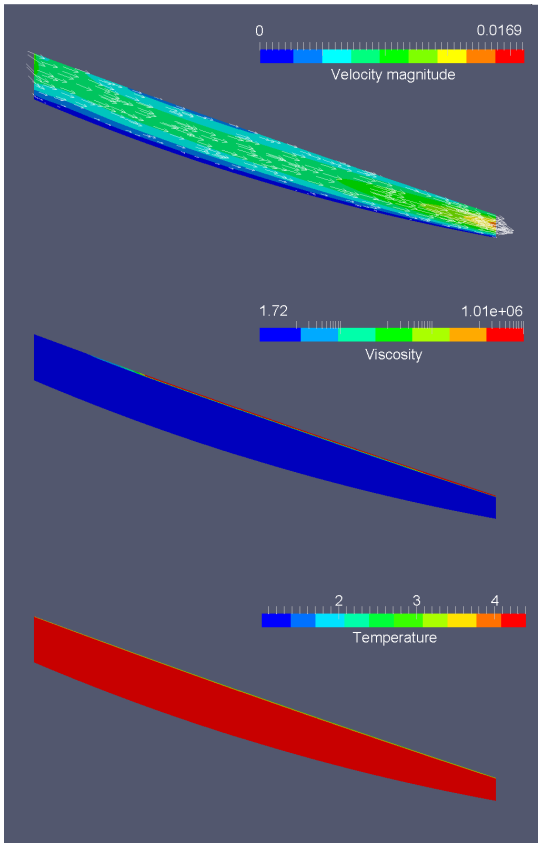

Nonlinear heat flow

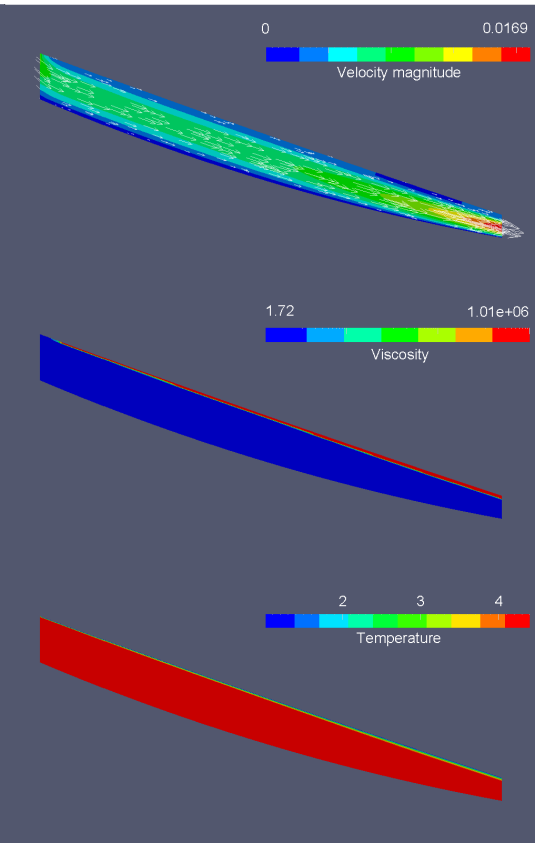

Linear heat flow

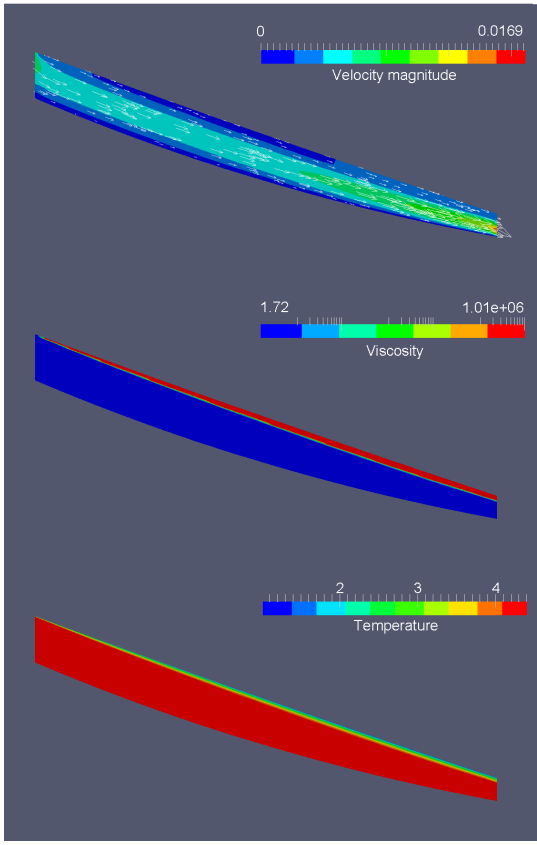

Nonlinear heat flow

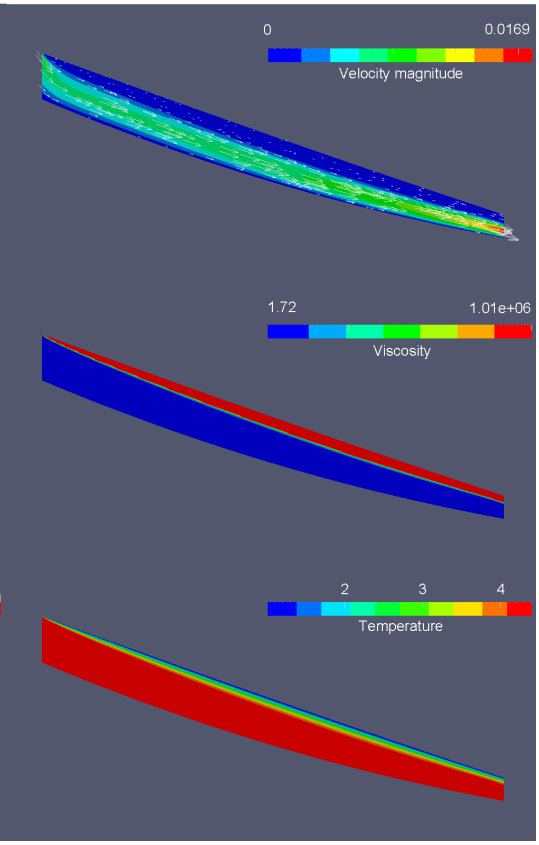

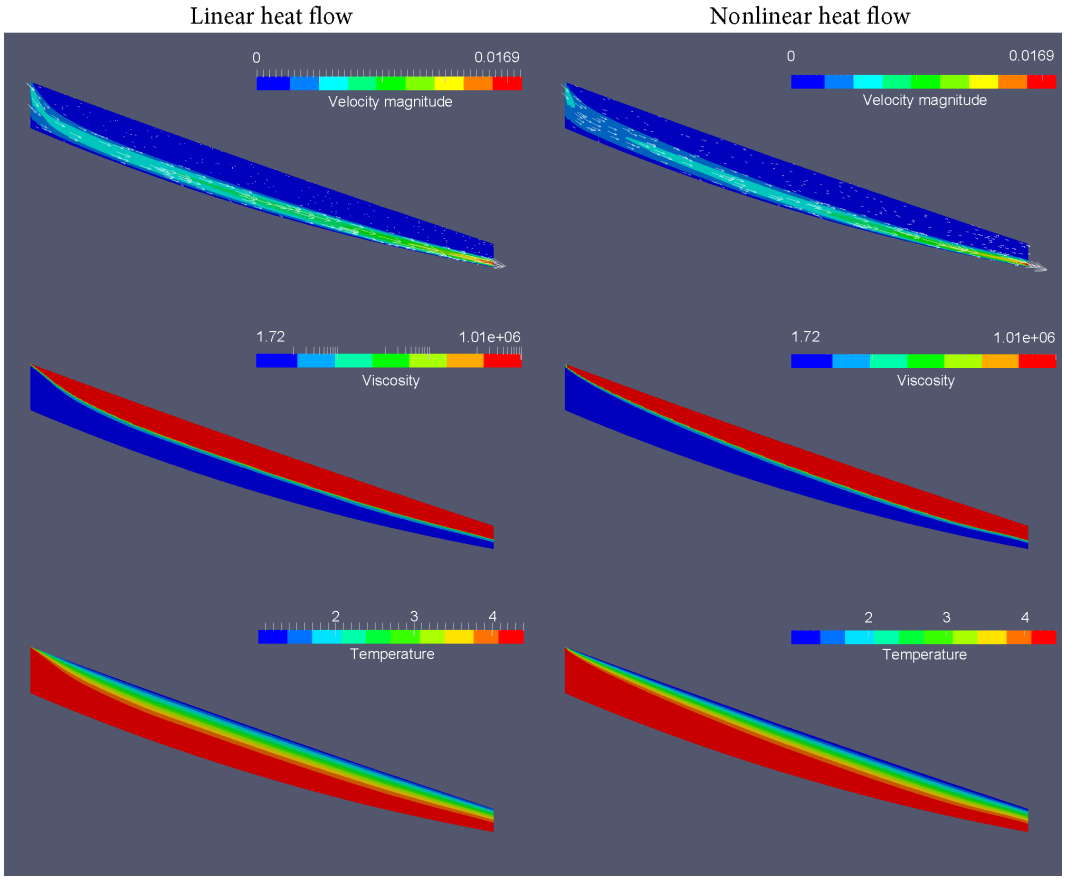

Fig. S1. Model dimensionless velocity magnitude, viscosity, and temperature in the case of linear (left panel) and nonlinear (right panel) heat transfer at the lava cooling surface with the atmosphere for the dimensionless effusion rate 10^{-2} (a), 10^{-3} (b), and 10^{-4} (c).

S2 No-slip condition at the lava interface with the atmosphere

We solve numerically the problem (1)-(14) with the following conditions at the boundary Γ_4. This boundary is divided into two parts by point D. We prescribe the free slip $\langle \mathbf{u}, \mathbf{n} \rangle = 0$, $\sigma \mathbf{n} - \langle \sigma \mathbf{n}, \mathbf{n} \rangle \mathbf{n} = 0$ at the circular arc connecting points D and E, and no-slip $\mathbf{u} = 0$ at the circular arc connecting points D and C. The thermal conditions from Eq. (15) and from Eq. (16) are used in the case of the linear and nonlinear heat flows at the entire boundary Γ_4, respectively. Dimensionless parameters used in Eqs. (15) and (16) are $Nu = 4$, a_1=2.593, and a_2=18.911. The numerical experiments have been performed for the dimensionless injection rate $|\mathbf{u}_1|$= 10^{-2} and smaller, and the dimensionless injection temperature is 4.4. The lava viscosity varies within six orders of magnitude, and $\eta_0 = 10^6$.

Figure S2 presents the results of modelling for linear (the left panels) and nonlinear (the right panels) heat flow: the dimensionless lava velocity magnitude (the upper panel), the logarithm ($\log_{10}$) of the dimensionless viscosity (the middle panel), and the dimensionless lava temperature (the lower panel). The lava temperature beneath the no-slip area decreases and the crust becomes much thicker there compared to the thinner crust beneath the free-slip area (also, compare to the case presented in Fig. S1a) at both linear and nonlinear heat flow at the cooling surface of the lava flow.

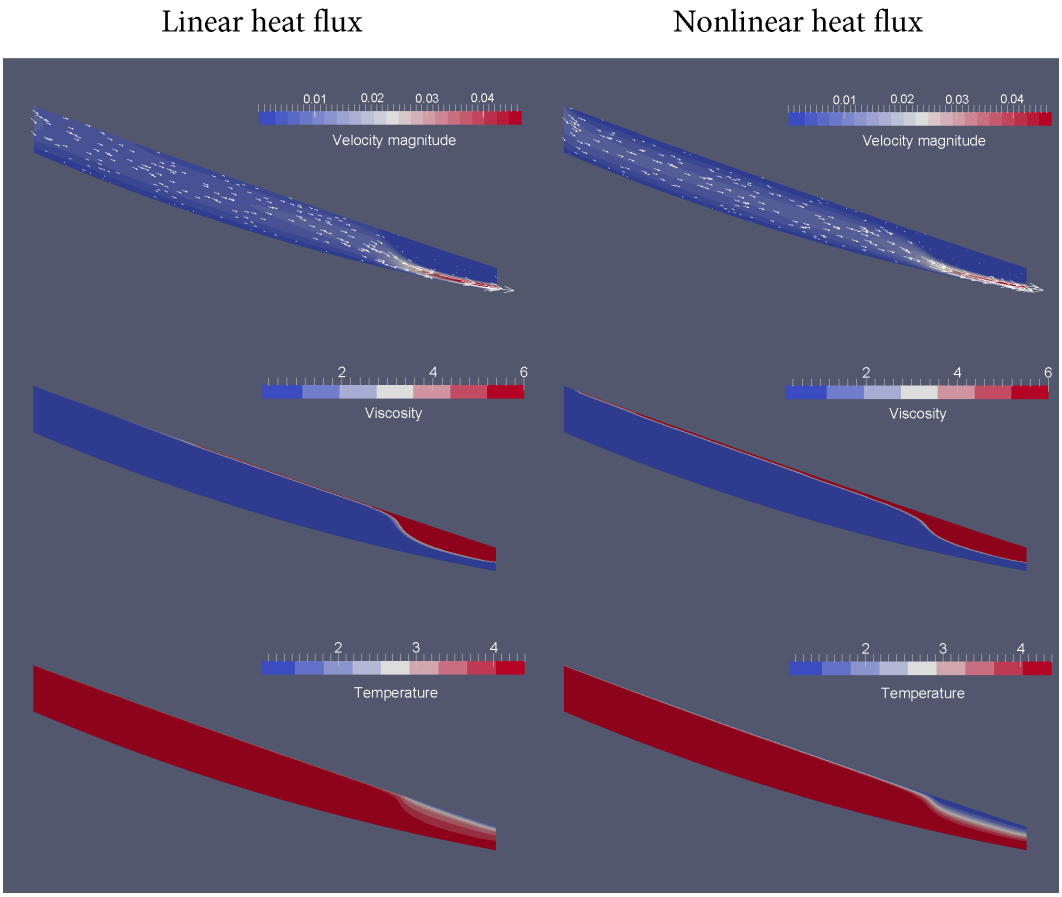

Fig. S2. Model dimensionless velocity magnitude, viscosity, and temperature in the case of linear (left panel) and nonlinear (right panel) heat transfer at the lava cooling surface with the atmosphere at the no-slip condition at the part of the interface between the lava flow and the atmosphere.

S3 Thermal conditions at the lava interface with the atmosphere

Data assimilation is based on the requirement of some physical parameters obtained as the solution of a mathematical model (e.g., temperature and heat flux from a lava flow model) to match their measurements (e.g., the temperature and heat flow at the interface of lava flow with the atmosphere). Normally, assimilations are tested using theoretical models employed in inversion schemes and synthetic data to be assimilated. Generating the synthetic data requires a theoretical model, which can be identical to, or different from, the one employed in the inversion scheme. In the case of using the same model to generate synthetic data and then to invert the data, an "inverse crime" is committed (Colton and Kress 1992).

To avoid the "inverse crime", synthetic data are normally perturbed, and numerical experiments are then performed to analyse how well the inverse problem can be solved (e.g., Korotkii et al. 2016). Another approach to avoid the "inverse crime" is to employ similar but different model to generate synthetic data. We employ in the data assimilation a model, which is different from one used in the inversion scheme, but similar in terms of fluid-dynamics description of lava flows. Hence, we solve numerically Eqs. (1)-(11) with the boundary conditions (12)-(15). We obtain hence the synthetic thermal data at the lava interface with the atmosphere. The computed heat flux $\varphi = -k\langle \nabla T, \mathbf{n} \rangle$ and temperature T_4 at boundary Γ_4 (Fig. S3) are then assimilated into the lava flow to constrain the condition at Γ_2 and determine lava temperature, viscosity and velocity.

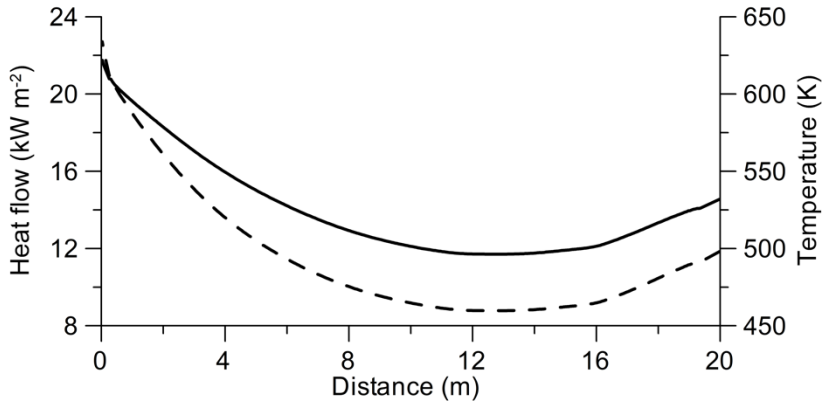

Fig. S3. Temperature (solid line) and heat flow (dashed line) at the interface of the lava flow and the atmosphere obtained from the solution of the direct problem (synthetic data for assimilation).

S4 The Navon et al. (1992) test

According to Korotkii et al. (2016), the gradient of the functional can be written in the form:

$$J(\xi+\chi)-J(\xi)=\int_{\Gamma_2}\chi\nabla J(\xi)\,d\Gamma+o(\|\chi\|),$$

where $\nabla J(\xi)=k(T_\xi)\left.\dfrac{\partial z}{\partial \mathbf{n}}\right|_{\Gamma_2}$. We have performed the χ-test by Navon et al. (1992) to verify the quality of the gradient of the cost functional with respect to the control variable. For this aim we choose the following increment $\chi=\varepsilon\nabla J(\xi)/\|\nabla J(\xi)\|$, where $\varepsilon=\|\chi\|$ is small. We rewrite then the last equation introducing a function of ε as

$$\nu(\varepsilon)=\frac{J(\xi+\varepsilon\nabla J(\xi)/\|\nabla J(\xi)\|)-J(\xi)}{\varepsilon\|\nabla J(\xi)\|}=1+O(\varepsilon).$$

For values of ε that are small but not too close to the machine zero, one should expect to obtain a value for $\nu(\varepsilon)$ that is close to 1. For $\xi=\xi^{(1)}\in\Xi$ (see the main text) the values of $\nu(\varepsilon)$ are shown in Fig. S4. For a value of ε between 10^{-2} and 10^{-7}, a near unit value of $\nu(\varepsilon)$ is obtained. This validates the quality of the adjoint model for use in obtaining the gradient of the cost function with respect to the control variable.

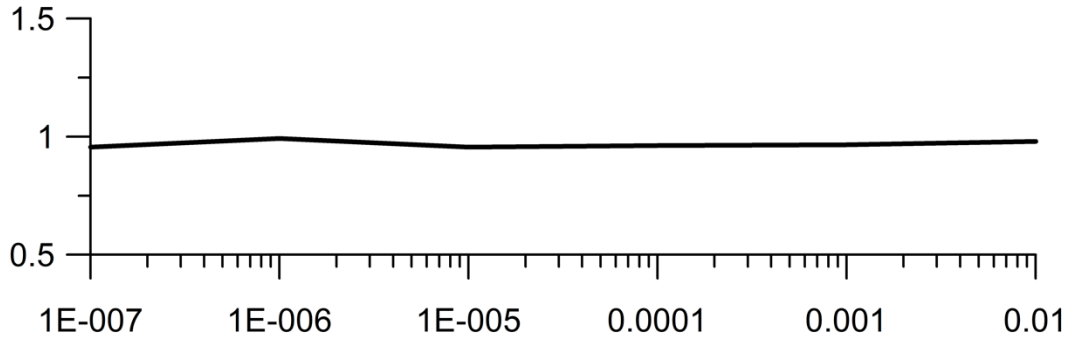

Fig. S4. Verification of the calculation of the gradient of the cost function *J* (Navon et al. (1992) test).

References

Colton, D., Kress, R., 1998. Inverse Acoustic and Electromagnetic Scattering Theory. Springer, Berlin. 110 pp.

Korotkii, A., Kovtunov, D., Ismail-Zadeh, A., Tsepelev, I., Melnik, O., 2016. Quantitative reconstruction of thermal and dynamic characteristics of lava from surface thermal measurements. Geophysical Journal International 205, 1767-1779.

Navon, I.M., Zou, X., Derber, J., Sela, J., 1992. Variational data assimilation with an adiabatic version of the NMC spectral model. Monthly Weather Review 120(7), 1433-1446.